JOURNAL OF SOLID STATE CHEMISTRY 63, 414–423 (1986)

Local Environment of Tungsten in Mixed Valence Tungsten Phosphate Glasses: An EXAFS Study

F. STUDER

Laboratoire de Cristallographie, Chimie et Physique des Solides, U.A. 251 ISMRa-Université, 14032 Caen Cedex, France

A. LEBAIL

Laboratoire des Fluorures et Oxyfluorures, U.A. 609 Université du Maine, 12047 Le Mans Cedex, France

AND B. RAVEAU

Laboratoire de Cristallographie, Chimie et Physique des Solides, U.A. 251 ISMRa-Université, 14032 Caen Cedex, France

Received June 24, 1985; in revised form October 4, 1985

The local order around tungsten atoms in some phosphotungstate glasses of the K_2O–P_2O_5–WO_{3-x} system was studied by EXAFS and X-ray diffusion techniques. From a previous work by EPR and optical spectra, an axially distorted octahedral environment was deduced around tungsten in these glasses. In agreement with this result, EXAFS shows that the structure of the phosphotungstate glasses is built up of distorted WO_6 octahedra joined by corners with PO_4 tetrahedra: long W–O distances can be associated with W–O–P bonds and short W–O distances with W–O–W bonds as was already observed in crystallized phosphotungstates. X-Ray diffusion shows that even for large WO_3 contents, WO_6 octahedra are predominantly joined by corners.

Introduction

Tungsten oxides are potential materials for electro-optical applications, owing to the ability of tungsten to take a mixed valence in many compounds. In this respect the recently synthesized tungsten phosphate glasses (*1*) could be of practical interest for realization of devices. Contrary to the crystallized phosphate tungsten bronzes belonging to the K_2O–P_2O_5–WO_{3-x} (*2–7*), for which X-ray diffraction and HREM studies have allowed an accurate structural determination, little is known about the local environment of tungsten in the glasses corresponding to this system. In a recent EPR and optical study (*1*) it was shown that in those glasses, the WO_6 octahedra were generally distorted (C_{4V}); the variation of the distortion, estimated from EPR lines (g values and linewidths), distinguishes the low tungsten content compositions in which tungsten octahedra seem to be isolated from the high tungsten contents where WO_6 octahedra would share corners or edges. Moreover, the drastic decrease of

0022-4596/86 $3.00

the intervalence band intensity in optical spectra, for potassium and tungsten (V) rich glasses, together with a weak constant and positive value of the magnetic susceptibility, led to the hypothesis of a local electron delocalisation in octahedral clusters.

Thus it appeared interesting to obtain more quantitative information especially about the interatomic distances in those amorphous materials. The main purpose was to study the first neighbors, oxygen and phosphorus atoms, around tungsten and in a second step the second coordination sphere and if possible the W–W distances. The present work deals with the EXAFS study of different glasses in the K_2O–P_2O_5–WO_{3-x} system. Moreover, little being known about the EXAFS behavior of tungsten in iono-covalent oxides, different crystallized tungsten oxides whose structure was known, have been studied as references.

Experimental Procedures

The synthesis of tungsten phosphate glasses has previously been described (*1*): homogeneous mixtures of K_2CO_3, $(NH_4)_2HPO_4$, and WO_3 were melted in air or under argon, in quartz crucibles, at temperatures ranging from 900 to 1600 K, according to the tungsten concentration. The glass was poured on a brass platelet heated at 600 K and then slowly cooled down to room temperature.

The EXAFS spectra at the tungsten L_{III} absorption edge (10, 200 eV) were recorded in LURE with the synchrotron radiation of DCI. The monochromator was a silicon monocrystal "channel cut." Absorption was deduced from the measurements of the intensity of the monochromatic beam in ionization chambers located before and after the sample (the energy step was taken equal to 1 eV). A value of 8991 eV for the maximum intensity at the K edge of copper was used as reference.

All the samples were prepared by sieving ground glasses over adhesive ribbon. A good compromise between the count statistics and the amplitude of the EXAFS modulations was found by changing the number of adhesive layers.

Methods of Analysis

The EXAFS modulations were analyzed using a standard method (*8*) with the aid of computer programs by A. Le Bail (*9*). From the EXAFS modulation of the form $\chi(k) = [u(k) - u_0(k)]/u_0(k)$, where $k(\text{Å}^{-1}) = (1/0.529)/[(E - E_0)^{1/2}/13.605]$ the continuous absorption background before the edge was estimated following the Victoreen formula (*10*) and substracted by interpolation beyond the edge. The resulting spectrum $u(k)$ was normalized by the atomic absorption coefficient $u_0(k)$ estimated by an approximated polynom and a smoothing of the curve until complete extinction of oscillations.

As a consequence of the rapid decrease of the amplitude of backscattering of oxygen with energy, the reduced amplitudes $\chi(k)$ were weighted by a k^3 factor. The module $|F(R)|$ of the Fourier transform of $f(k) = k^3\chi(k)$ was calculated between the limits k_{min} and k_{max} where the amplitudes of $f(k)$ were close to zero.

The partial functions $f_j(k)$ associated with the coordination sphere of order j were estimated by an inverse Fourier transform of $F(R)$ in the interval (R_{min}, R_{max}) deduced from the moduls of $F(R)$.

The filtered spectra were approximated by the relation (*11*)

$$f_j(k) = (k/R_j)^2 N_j \text{So}^2(k) T_j(k) \, e^{-2\sigma_j^2 k^2} e^{-2R_j/\lambda(k)} (\sin(2kR_j + \phi_j(k)) \quad (1)$$

in which R_j is the mean radius of the coordination sphere, N_j is the number of backscattering centers, So^2 is the multielectronic factor (used as a scaling factor), T_j is the backscattering amplitude, σ_j is the standard

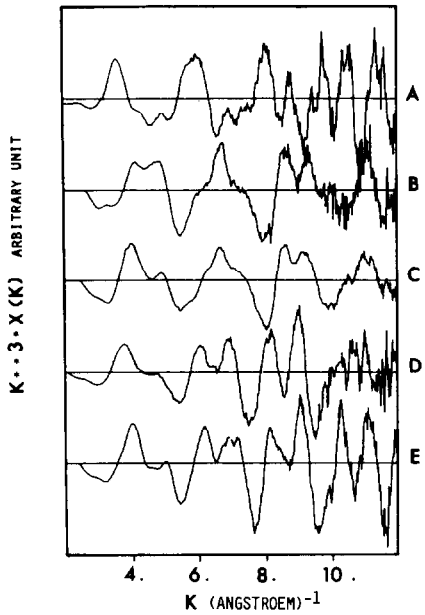

FIG. 1. The $k^3\chi(k)$ modulations in the case of some oxides chosen as references: (A) $Na_{0.65}WO_3$, cubic tungsten bronze, regular octahedron; (B) $CaWO_4$, scheelite, regular tetrahedron; (C) WO_3, monoclinic form, distorted WO_6 octahedron; (D) $CuWO_3$, triclinic; (E) $NiWO_4$, tetragonal symmetry.

deviation of the distances distribution, $\lambda(k)$ is the electron mean free path approximated by $\lambda = k/\Gamma$, and ϕ_j is the total phase shift.

In expression (1), theoretical amplitudes and phase shifts calculated by Teo and Lee (*12*) have been used to fit the spectra. The electron mean free path λ corresponding to a Γ value of 0.6 $Å^{-2}$ was found to give the best results on reference compounds.

For testing the Teo and Lee parameters, R_j, σ_j, and So^2 (for a given N_j) were fitted by a least square method in the case of crystallized tungsten oxides, the value of the edge energy Eo being adjusted to the best fit. This last point allowed a good correction for the differences between phase shifts calculated for neutral atoms and real ones observed in the case of ions.

In the case of glasses, the fitting of N_j, R_j, and σ_j parameters would suppose a good transferability of So^2 values of crystallized compounds. As this last point was difficult to achieve and the number of first neighbors around tungsten was estimated from other methods to be equal to 6, the R_j, σ_j, and So^2 parameters were also fitted in glasses.

A systematic effect of phase shift is to move the peak positions some tenths of angstroms to the lower values. Moreover, the steep limits of the Fourier integral give rise to unexpected oscillations which can be removed by the use of a Gaussian window $G(k) = \exp\{-A(k - k_0^2)\}$ where k_0 is the center of the (k_{min}, k_{max}) interval and A is chosen so that $G(k_{max}) = 0.1$ (*13*).

All the spectra shown in this work will correspond to the modulus $|F'(R)|$ of the Fourier transform of the $G(k)f(k)$ EXAFS modulations corrected for the phase shift of the fist W–O pairs.

Results and Discussion

Reference Oxides

The response of EXAFS to tungsten in iono-covalent compounds and especially in oxides has not been studied up to the present, as far as we know. For this reason several oxides whose structure was known with accuracy were chosen. In these oxides different coordinations are observed: regular tetrahedral in $CaWO_4$ (*14*), or almost regular octahedral in the perovskite tungsten bronze $Na_{0.64}WO_3$ (*15*), or distorted octahedral in different ways in $NiWO_4$ (*16*), $CuWO_4$ (*17*), and WO_3 (*18*).

The $k^3\chi(k)$ modulations corresponding to these reference oxides are presented in Fig. 1 and the modulus $|F'(R)|$ are shown on Fig. 2. The results of the least square refinements of R_j, σ_j, and So^2 are presented in Table I for oxygen nearest neighbours and in Table II for some second and third neighbors. In these tables, the X-ray diffraction data are also given.

First neighbors. A direct comparison of R_1 distances (Table I) shows that the agreement between EXAFS determination and

TABLE I

CRYSTALLOGRAPHIC DATA AND EXAFS PARAMETERS FOR THE FIRST COORDINATION SPHERE (W–O PAIRS) OF SOME CRYSTALLIZED REFERENCE COMPOUNDS

Compounds	R (Å) RX	R (Å) EXAFS	σ (Å) EXAFS	R_W (%)	So^2	N RX	N EXAFS
$CaWO_4$	1.750	1.77	0.062	9	0.677	4	4
$Na_{0.65}WO_3$	1.920	1.90	0.0833	10	1.006	6	6
WO_3	1.732–1.800	1.77	0.061	6	0.510	2	4.6
	1.867–1.948	—				2	
	2.066–2.190	2.13	0.035	9		2	1.4
$NiWO_4$	1.80	1.81	0.058	7.5	0.561	4	4.3
	2.20	2.20	−0.025	10.5			1.7
$CuWO_4$	1.763	1.81	0.047	15		1	4.6
	1.815–1.846	—			0.410	2	
	1.988–2.026	—				2	
	2.207	2.21	0.032	10		1	
W_{metal}	2.741	2.75	0.052	12.5	0.75	8	8

crystallographic data is quite good for simple coordinations, i.e., regular WO_4 tetrahedra in $CaWO_4$, regular WO_6, octahedra in $Na_{0.65}WO_3$. These results are in agreement with those observed by different authors for metallic tungsten, which exhibits a cubic coordination. For other oxides the interpretation of the EXAFS spectra is more complex.

In the case of $NiWO_4$, the axial distortion of the WO_6 octahedra led to a split in two oxygen subshells (0.4 Å apart) hardly visible on Fig. 2E but much more separated without the correction of the termination effect so that they could be simulated independently. A good agreement between structural data and EXAFS distances is still observed but the number of oxygen atoms in each subshell has been determined within a 20% error.

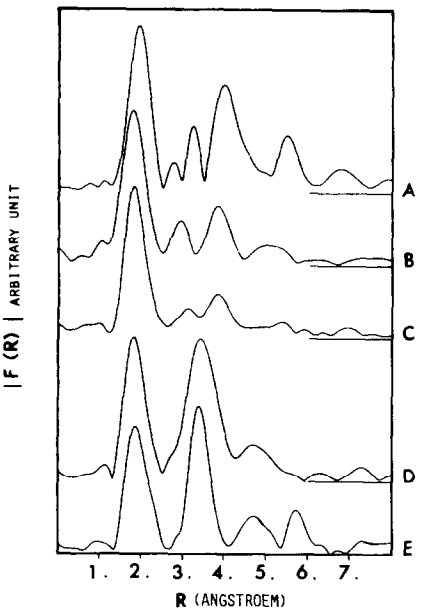

FIG. 2. Transformed EXAFS spectra $|F'(R)|$ corrected for (W–O) phase shift and truncatured for the same reference compounds (see Fig. 1 legend).

TABLE II

CRYSTALLOGRAPHIC DATA AND EXAFS PARAMETERS FOR FURTHER NEIGHBORS CORRESPONDING TO W–A PAIRS (WITH A = Na, W, O) IN THE REFERENCE COMPOUNDS

Compounds	Type of pairs	R (Å) RX	R (Å) EXAFS	σ (Å)	R_W (%)	So^2	N RX
$CaWO_4$	W–O	3.00	2.99	0.015	10	0.584	4
$Na_{0.65}WO_3$	W–Na	3.29	3.28	0.036	11	0.70	6.5
	W–W	3.837	3.69	0.059	21	0.86	6
	W–W	5.420	5.41	0.065	26	1.11	12
WO_3	W–W	3.713					
		to	3.72	0.10	16	1.05	6
		3.880					
W_{metal}	W–W	3.165	3.19	0.014	19	0.4	6
	W–W	4.747	4.51	0.067	27	1.02	12

For less symmetrical structures, such as WO_3 and $CuWO_4$, several crystallographic sites are involved, so that the W–O distances spread over rather wide ranges. The Figs. 2C and D, which are characterized by a main peak centered on the average small W–O distances and exhibit a weak shoulder corresponding to longer W–O distances, are in agreement with the X-ray data. This phenomenon is similar to the one observed in disordered materials and is correlated with a reduction of EXAFS amplitudes: as a matter of fact the So^2 values of WO_3 and $CuWO_4$ are the weakest of the references. In a first approximation, a resolution in two subshells was found possible also for both less symmetric compounds.

A comparison of So^2 factors shows that they spread over a wide range depending on type of structure and tungsten environment. The other causes of this dispersion are likely experimental (inhomogeneities, too large thickness of samples) but may also be related to differences in chemical environment, ionicity, or electronic configuration.

For all crystallized compounds, the edge energy calculated from the position of the half height of the edge peak, stands around 10,197 ± 2 eV. No significant deviation from this mean value could be observed with the ionization state of tungsten (from metallic state to W^{6+} ion) within the experimental precision (1 eV).

Further neighbors. Some further neighbors could be identified without ambiguity (Table II). $Na_{0.65}WO_3$ was found to be the most favorable case: W–Na and W–W pairs were easily observed at $a_p\sqrt{\frac{3}{2}}$, a_p, and $a_p\sqrt{2}$, respectively. However, contrary to the Na–W distance which is found to be very close to that observed by X-ray diffraction, the EXAFS W–W distance is 0.147 Å smaller than that obtained by X ray. This different result obtained by EXAFS can be explained by a shadowing effect with a consequently large perturbation on phase shift due to the oxygen contribution. It can be noted that the 24 oxygen atoms expected at 4.29 Å are hardly visible owing to the fast decrease of their backscattering amplitude and large anisotropic thermal vibration (the ellipsoid being probably an elongated disk perpendicular to the W–W bond axis as in fluoride perovskite).

On Fig. 2B, the second peak for $CaWO_4$ can be attributed unambiguously to four oxygen neighbors but the third one is a combination of Ca and W contributions which could not be separated. Apart from metallic tungsten where many W–W pairs could be identified, the W–W pairs were only visible in the case of WO_3.

In $NiWO_4$ and $CuWO_4$ compounds, the large and intense peak observed between 3 and 4 Å is the result of the contribution of W–W and W–Ni or W–Cu pairs.

Glasses

On Fig. 3 are presented the $k^3\chi(k)$ spectra for a series of glasses with the same K_2O

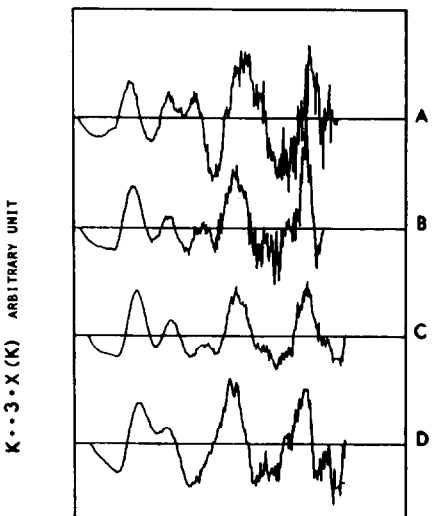

FIG. 3. The $k^3\chi(k)$ modulations for some glasses with 30 mole% K_2O and increasing WO_3 contents (for notation see text and Table III). Oscillations above 10 $Å^{-1}$ are lost in the background and insignificant.

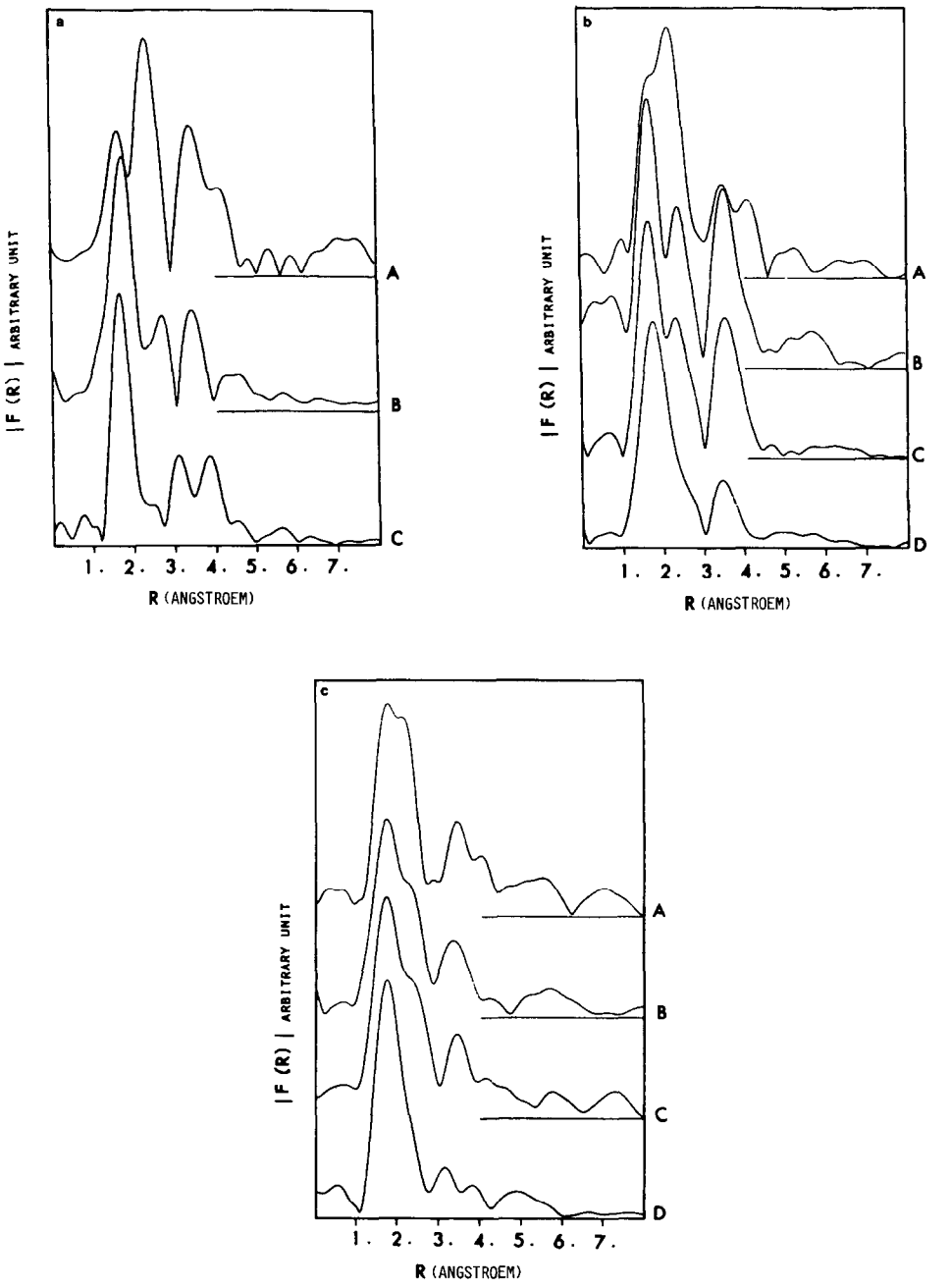

FIG. 4. Transformed EXAFS spectra for phosphotungstate glasses containing (a) 10 mole% K_2O; (b) 30 mole% K_2O; and (c) 40 mole% K_2O. The letters on the figures refer to compositions given in Table III. On Figs. 4b and c, spectra B and C refer to the same global composition, but with very different W^V contents.

TABLE III

EXAFS PARAMETERS FOR THE FIRST OXYGEN NEIGHBORS DISTRIBUTED IN TWO SUBSHELLS, AND FOR THE SECOND PHOSPHORUS NEIGHBORS IN PHOSPHOTUNGSTATE GLASSES[a]

	Compositions (%)										
	K_2O	P_2O_5	WO_{3-x}	% W^{5+}		R (Å)	σ (Å)	R_W (%)	$(So^2)_O$ 6 neighbors	pN	$(So^2)_P$ 4 neighbors
A		45	45	3.0	W–O	1.66	0.110	10		2.5	
					W–O	2.13	0.100	10	0.458	3.5	
					W–P	3.27	0.1464	5			1.806
B	10	20	70	0.1	W–O	1.80	0.054	10		4.8	
					W–O	2.22	0.027	14	0.308	1.8	
					W–P	3.40	0.0917	6			0.834
C		15	75	0.1	W–O	1.71	0.085	11		4.6	
					W–O	2.06	0.078	8		1.4	
A		55	15	11.0	W–O	1.61	0.060	17		1.4	
					W–O	2.09	0.056	19	0.530	4.6	
					W–P	3.33	0.113	11			1.20
B		25	45	86.0	W–O	1.72	0.056	9		3.0	
	30				W–O	2.19	0.040	8	0.362	3.0	
					W–P	3.40	0.100	6			1.22
C		25	45	0.3	W–O	1.72	0.056	9		3.0	
					W–O	2.18	0.040	8	0.309	3.0	
					W–P	3.41	0.142	8			1.97
D		10	60	0.1	W–O	1.78	0.060	14		4.8	
					W–O	2.24	0.032	4	0.352	1.2	
					W–P	3.47	0.055	13			0.394
A		40	20	0.7	W–O	1.68	0.054	10		2.2	
					W–O	2.15	0.050	11	0.419	3.8	
					W–P	3.36	0.110	10			1.126
B		20	40	20.0	W–O	1.77	0.042	10		2.9	
	40				W–O	2.22	0.044	8	0.378	3.1	
					W–P	3.39	0.149	14			1.82
C		20	40	0.1	W–O	1.75	0.064	12	0.408	3.1	
					W–O	2.27	0.062	9	0.408	2.9	
					W–P	3.41	0.094	6			1.0
D		15	45	18.0	W–O	1.75	0.050	13		4.1	
					W–O	2.25	0.052	6	0.328	1.9	

[a] The numbers of oxygen in both subshells have been estimated from the scaling factors So^2.

concentration (30 mole% K_2O). The less correct statistic than in reference compounds (Fig. 1) comes from the smaller tungsten concentration. Thus, the Fourier transforms were calculated in a more limited k range ($k \leq 10$ Å^{-1}). On Figs. 4a–c are presented the modulus of the Fourier transforms $|F'(R)|$ for three series of glasses with varying K_2O concentration. On all spectra at least three to four peaks more or less resolved, are visible up to 4 Å.

First neighbors. The first oxygen neighbors of tungsten are expected to be located at distances ranging from 1.5 to 2.5 Å. If one excepts the highest tungsten concentration, the systematic splitting of the first peak was interpreted as a distribution of the oxygen first neighbors between two subshells. The numbers N of oxygen atoms in each subshell are reported in Table III. They were deduced from the So^2 scaling factors on the basis of a sixfold coordina-

TABLE IV

DISTANCES BETWEEN TUNGSTEN SITES AND SURROUNDING ATOMS IN A TYPICAL PHOSPHOTUNGSTATE CRYSTALLIZED COMPOUND (FROM (6)) AS DEDUCED FROM X-RAY DIFFRACTION

	$K_{0.5}P_2W_4O_{16}$ R (Å)				
Sites	W–O	W–P	W–W	W–K	W–O 2nd neighbors
W_1	1.81 × 2		3.756 × 2	3.92	
	1.842		3.736	3.795 × 2	3.861 to 4.42
	2.015	3.351		4.06	
	2.025 × 2	3.512 × 2			
W_2	1.875 × 2		3.75 × 2		
	1.899		3.736		
	1.960 × 2		3.756 × 2		
	1.990	3.667			

tion around tungsten ions in agreement with EPR and optical results. The error on the determination of N was estimated to ±0.5. The distances corresponding to both subnetworks ranged between 1.61 and 2.27 Å (Table III).

These distances are in agreement with those observed by EXAFS and X-ray diffraction in the reference compounds characterized by a distorted octahedral coordination (WO_3, $NiWO_4$, and $CuWO_4$). A more detailed analysis of Table III leads us to distinguish two groups of W–O distances: short W–O distances ranging from 1.6 to 1.9 Å, and longer W–O distances greater than 2 Å. It must be pointed out that the number of long W–O distances (>2 Å) increases as the phosphorus content increases. This is in agreement with the Pauling's rule: the longest W–O distances correspond indeed to W–O–P bonds whereas the short ones characterize either W–O–W distances or a "free oxygen" only linked to one tungsten atom.

This type of distribution of W–O distances between two subshells is characteristic of a distorted octahedral environment. It can be compared to the structural results previously observed in the phosphate tungsten bronzes (*2–7*) as shown in Table IV for comparable WO_3/P_2O_5 ratios. However, one can see that in this latter case the differences between the two groups of distances is not so large because of the electronic delocalization in the whole octahedral framework.

Thus it appears as most probable that for high tungsten contents (see Table III compositions 10, 15, 75; 30, 10, 60; and 40, 15, 45) each WO_6 octahedron will share its corners with only one or two PO_4 tetrahedra involving only one or two W–O–P bonds per octahedron. On the contrary, for high P_2O_5 contents each WO_6 octahedron shares its corners with five PO_4 tetrahedra (see, for instance, composition 30, 55, 15, Table III) or four PO_4 tetrahedra (see compositions 40, 40, 20) involving five and four W–O–P bonds per octahedron, respectively. Moreover in the case of octahedra sharing their corners with five tetrahedra, the remaining very short W–O distance (1.61 Å for 30, 55, 15) suggests that the sixth oxygen atom of the octahedron is not shared with the other polyhedra of the glass. It results in a tendency to form a tungstyl ion which is to be compared to the molybdenyl encountered in several structures (*19–20*). This very

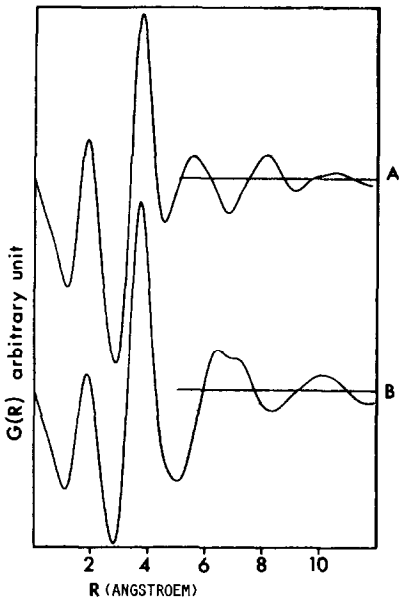

FIG. 5. Reduced distribution function obtained from X-ray diffusion spectra of two tungsten-rich glasses.

short W–O bond was also previously deduced from the analysis of the *d–d* transitions in optical spectra and from the variations of local distortion in EPR spectra of these glasses (*1*). This tendency to form a short W–O bond was also observed by X-ray diffraction for several crystallized phosphotungstate (*7*).

A systematic decrease of the So^2 parameters as the tungsten concentration increases (Table III) has been observed for each series of glasses: it can reach quite smaller values than in the less symmetrical reference structures. This result can be related either to a more disordered tungsten environment in glasses, as was noticed in the analysis of the scaling factor, or to an effective decrease of the coordination number, especially in the case of the highest tungsten concentration (10, 15, 75).

One could also think of a continuous evolution between a distorted octahedral environment (4 + 2) to a tetrahedral one with four further oxygens at 3 Å like in $CaWO_4$ compound. It is not possible to decide between these hypothesis.

Further neighbors. Except for the lowest P_2O_5 concentration, the third peak on $F'(R)$ (Fig. 4) has been assigned to W–P pairs. The fitting of the associated EXAFS modulation led to a reliability factor less than 10% and to W–P distances coherent with those commonly observed in crystallized phosphotungstates (Table IV). In all cases, an increase of W–P distances appeared to be correlated with the increase of long W–O distances.

A fourth peak has been observed at high P_2O_5 concentration as well as at high WO_3 content (Figs. 4a,b). In the P_2O_5 rich glasses, it may result from the contribution of W–O pairs coming from the three other oxygens of the PO_4 groups, at distances ranging from 3.8 to 4.2 Å and from W–K pairs also around 3.8 Å (Table IV). In the tungsten-rich glasses, the W–W pairs 3.8 Å may also contribute to the intensity of this peak together with W–O and W–K pairs, depending on the K_2O concentration.

For distances greater than 3.5 Å, the number of pairs which contribute to the EXAFS modulations is too important to allow a direct and accurate determination. To localize the W–W pairs, a preliminary X-ray diffusion study was realized on two glasses (30, 10, 60 and 10, 20, 70) (Fig. 5), characterized by a high tungsten concentration. The reduced distribution function presented in Fig. 5 shows in both cases a first peak near 1.9 Å and a large second one at 3.74 Å which can be assigned to W–O pairs and W–W pairs, respectively, since the W diffusion factor largely predominates. The distance of 3.74 Å is consistent with WO_6 octahedra sharing corners.

It is worth noting that the long-range order appears to be completely different in both cases, due probably to the large variation of K_2O concentrations.

Conclusion

The EXAFS and X-ray diffusion study of the phosphate tungsten glasses of the system K_2O–P_2O_5–WO_{3-x} shows that their structure is built up from distorted WO_6 octahedra sharing their corners with PO_4 tetrahedra. From the analysis of the interatomic distances it appears that the distortion of the octahedra depends on the number of W–O–P bonds per octahedron: this phenomenon is directly correlated to the P_2O_5 content in the glass. For tungsten-rich glasses, the X-ray diffusion study shows clearly that WO_6 octahedra share their corners. No evidence of edge-sharing WO_6 octahedra was found, neither by EXAFS nor by X-ray diffusion, at least in a regular ordering; this result is in agreement with the Zachariasen rules.

References

1. N. Rih, Thèse de 3e cycle. Université de Caen, (1983).
2. J. P. Giroult, M. Goreaud, Ph. Labbe, and B. Raveau, *J. Solid State Chem.* **44,** 407 (1982).
3. J. P. Giroult, M. Goreaud, Ph. Labbe, and B. Raveau, *Acta Crystallogr. Sect. B* **37,** 2139 (1981).
4. J. P. Giroult, M. Goreaud, Ph. Labbe, and B. Raveau, *Acta Crystallogr. Sect. B* **38,** 2342 (1982).
5. M. Goreaud, Ph. Labbe, and B. Raveau, *Acta Crystallogr. Sect. B* **36,** 15 (1980).
6. M. Goreaud, Ph. Labbe, and B. Raveau, *J. Solid State Chem.* **56,** 41 (1985).
7. P. Kierkegaard, *Ark. f. Kem.* **19,** 4 (1962).
8. D. Raoux, J. Petiau, P. Bondot, G. Calas, A. Fontaine, P. Lagarde, P. Levitz, G. Loupias, and A. Sadoc, *Rev. Phys.* **15,** 1079 (1980).
9. A. Le Bail, C. Jacoboni, and R. de Pape, *J. Solid State Chem.* **52,** 32 (1984).
10. "International Tables for X-ray Cristallography" (K. Lansdale, ed.), Kynoch Press, Birmingham, England.
11. E. A. Stern, B. A. Bunker, and S. M. Heald, *Phys. Rev. B* **21,** 5521 (1980).
12. B. K. Teo and P. A. Lee, *J. Am. Chem. Soc.* **101,** 2815 (1979).
13. S. J. Gurman and J. B. Pendry, *Sol. State Commun.* **20,** 287 (1976).
14. R. W. G. Wyckoff, "Crystal Structures," Vol. 3, p. 19. Interscience, New York, 1976.
15. A. Magneli and B. Blomberg, *Acta Chem. Scand.* **5,** 372 (1951).
16. R. O. Kelling, *Acta Crystallogr.* **10,** 209 (1957).
17. L. Kihlborg and E. Gebert, *Acta Crystallogr. Sect. B* **26,** 1020 (1970).
18. B. O. Loopstra and H. M. Rietveld, *Acta Crystallogr. Sect. B* **25,** 1420 (1969).
19. A. Leclaire, J. C. Monier, and B. Raveau, *J. Solid State Chem.* **48,** 147 (1983).
20. A. Leclaire, J. C. Monier, and B. Raveau, *Acta Crystallogr. Sect. B* **40,** 180 (1984).